Maximum wave-power absorption under motion constraints associated with both controlled and uncontrolled degrees of freedom

Maximum wave-power absorption under motion constraints associated with both controlled and uncontrolled degrees of freedom

A. Cotten, D. I. M. Forehand

Institute of Energy Systems, School of Engineering, University of Edinburgh

Abstract

A semi-analytical method is derived, which enables optimisation of the power absorption of a collection of wave-interacting bodies, subject to a weighted global motion constraint associated with both the controlled and uncontrolled modes of motion. As an illustrative example, the method is then applied to a six degree of freedom solo duck with various modes of motion under direct control. This is in order to highlight the benefits of employing the extended constraint and to explore the dependence of the existence of a solution on the physical properties of the system. The method is also used to investigate the effects of conceding control of certain degrees of freedom on the capture width ratio of the solo duck.

Keywords: Complex conjugate control, linear hydrodynamics, motion constraints, optimal control, wave energy converter

1. Introduction

Under the assumptions of linear radiation-diffraction theory, it is well known that the optimal power that can be absorbed by a wave energy device in regular seas can be expressed mathematically, in terms of the hydrodynamic coefficients (e.g. [1]). For the purposes of achieving the body motions necessary for optimal power, the required control forces can also be expressed in terms of the hydrodynamic properties of the absorber (e.g. [2]). The technique is often termed 'complex conjugate control', since the fundamental result is that the optimum power take-off impedance is equal to the complex conjugate of the intrinsic impedance.

However, for wavelengths that are large relative to the body, the demanded excursions can greatly exceed the bounds of validity of linear theory. In order to maintain results in accordance with the linearity assumptions, Evans [3] used a method of Lagrange multipliers to optimise the absorbed power subject

Email addresses: Alfred.Cotten@ed.ac.uk (A. Cotten), D.Forehand@ed.ac.uk (D. I. M. Forehand)

to a global constraint (proportional to the wave amplitude) on the body motions. Pizer [4] then extended that method so that the global constraint could encompass different weightings for each degree of freedom, each of which were independent of the wave amplitude. One application of that theory investigated the performance of a solo duck, with a variety of sets of controlled degrees of freedom (DoFs), with motions prohibited in the other directions. In practice, it may be more economical to allow free motion in the uncontrolled DoFs instead of imposing rigid constraints. By extending the theory to allow uncontrolled DoFs, Pizer [5] investigated various combinations of free (controlled and uncontrolled) and fixed DoFs for solo ducks with DoFs only in the plane perpendicular to the incoming wavefronts. However, the motion constraints in those models only applied to the controlled DoFs. This leaves the possibility of unrealistic motions in the uncontrolled DoFs that violate the assumptions of the linear theory.

A small number of subsequent publications have utilised the same approach as [4] to optimise power absorption subject to a motion constraint [6][7], and there even exist examples of the use of multiple constraints in order to individually constrain multiple degrees of freedom, whilst maximising power absorption [8][9]. However, to the authors' knowledge, there have been no further publications since [5] that consider complex conjugate control in the presence of uncontrolled degrees of freedom.

The work presented herein extends the theory of Pizer [4][5] to optimise the power absorption subject to motion constraints on all DoFs, exploiting the hydrodynamic, hydrostatic and inertial coupling between the controlled and uncontrolled DoFs. To act as a precursor for the main results of this paper, Section 2 first presents explicitly the theory that was introduced in [5], which covers the application of complex conjugate control to a set of controlled and uncontrolled degrees of freedom, with a motion constraint applied to just the controlled degrees of freedom. This theory is then extended in Section 3, with the application of the motion constraint to all the degrees of freedom. The properties of the resulting equations are then investigated with regards to obtaining numerical solutions in Section 4. (Whilst the theory presented in Sections 3 and 4 is intended to be self-contained, contrasting it with the foundational theory set out in [4] may provide the reader with a useful perspective.) The introduced theory is then applied to a solo duck wave energy converter in Section 5, with emphasis both on crucial aspects of the theory itself, and features of the device that may aid in its future development. The main results are then summarised in Section 6. Despite the theory being applicable to a collection of bodies with any number of degrees of freedom (including jointed bodies), the solo duck is better able to illustrate some of the crucial aspects of the new theory.

2. Formulation with uncontrolled DoFs

The formulation of constrained complex conjugate control presented in [4] requires control of all the degrees of freedom. More specifically, it requires that damping and stiffness forces can be applied to all DoFs in order to extract (or

inject) power. For systems in which power can only be extracted from certain DoFs and not from others, the equations of motion can be rearranged such that the same method can be applied to only the controlled (power-extracting) DoFs. Whilst this treatment to handle uncontrolled or released DoFs is introduced and applied to three DoF solo duck systems in [5], it is useful to review some of the key results. In the rest of this paper, the power-extracting modes will be referred to as 'controlled', whilst the uncontrolled modes through which power cannot be transferred will be referred to as 'free' or 'uncontrolled'. Degrees of freedom may also be referred as 'modes' of motion.

A system with N degrees of freedom oscillating in monochromatic waves of period, T, and amplitude, A, is considered. We assume that between 1 and $N-1$ of these DoFs are controlled, with the remaining free. It is beneficial to represent the equations of motion of such a system in terms of the controlled DoFs and the free DoFs (Eq. 1, [5]).

$$\begin{bmatrix} \mathbf{F}_c \\ \mathbf{0} \end{bmatrix} = \begin{bmatrix} \mathbf{Z}_{cc} & \mathbf{Z}_{cf} \\ \mathbf{Z}_{fc} & \mathbf{Z}_{ff} \end{bmatrix} \begin{bmatrix} \mathbf{U}_c \\ \mathbf{U}_f \end{bmatrix} - A \begin{bmatrix} \mathbf{X}_c \\ \mathbf{X}_f \end{bmatrix} \tag{1}$$

where A is the wave amplitude, subscripts c and f are used to denote components relating to the controlled and uncontrolled modes, respectively, $\mathbf{X}$ denotes excitation forces, $\mathbf{F}$ the control forces, and $\mathbf{Z}$ is the intrinsic impedance defined relative to the velocities, $\mathbf{U}$.

It is necessary to use the control forces to optimise the controlled velocities, $\mathbf{U}_c$, in order to maximise power extraction. However, hydrodynamic, hydrostatic and inertial coupling between the controlled and free DoFs encapsulates a dependence of the motions of the controlled modes on the motions of the free modes. The equations of motion of the free modes can be used to rewrite the equations of motion of the controlled modes (Eqs. 2, 3, 4, [5]), using the superscript, m, to distinguish the modified quantities from their counterparts in the original equations of motion (Eq. 1). $\mathbf{C}$ is the control matrix, which can be of particular relevance to the practical realisation of such control techniques.

$$\mathbf{F}_c = \mathbf{Z}^m_{cc}\mathbf{U}_c - A\mathbf{X}^m_c = -\mathbf{C}\mathbf{U}_c \tag{2}$$

where

$$\mathbf{Z}^m_{cc} = \mathbf{Z}_{cc} - \mathbf{Z}_{cf}\mathbf{Z}^{-1}_{ff}\mathbf{Z}_{fc} \tag{3}$$

and

$$\mathbf{X}^m_c = \mathbf{X}_c - \mathbf{Z}_{cf}\mathbf{Z}^{-1}_{ff}\mathbf{X}_f \tag{4}$$

As stated in [5], Eq. 2 can then be subjected to the same method presented in [4], provided that the motion constraint applies only to the controlled modes of motion. Specifically, the power can be expressed in terms of the controlled velocities and hydrodynamic properties (Eq. 5), where * denotes the complex conjugate transpose, and $\mathbf{B}_{cc}$ is the real part of $\mathbf{Z}^m_{cc}$.

$$\mathbf{P}(\mathbf{U}_c) = \frac{A^2}{8}\mathbf{X}^{m*}_c\mathbf{B}^{-1}_{cc}\mathbf{X}^m_c - \frac{1}{2}(\mathbf{U}_c - \frac{A}{2}\mathbf{B}^{-1}_{cc}\mathbf{X}^m_c)^*\mathbf{B}_{cc}(\mathbf{U}_c - \frac{A}{2}\mathbf{B}^{-1}_{cc}\mathbf{X}^m_c) \tag{5}$$

The controlled velocities that are optimal under the motion constraints comprise an additional damping term, which is a function of μ, a Lagrange multiplier, and $\mathbf{\Gamma}_c$, the diagonal matrix of constraint weightings, which are expressed relative to the velocities. Under certain wave conditions, the constraint may not be active, in which case the multiplier vanishes, reducing the optimal velocities to their unconstrained optimal form, which can be deduced by inspection of Eq. 5.

$$\mathbf{U}_c^{opt} = \frac{A}{2}(\mathbf{B}_{cc} + \mu\mathbf{\Gamma}_c^{-2})^{-1}\mathbf{X}_c^m \tag{6}$$

By substituting these optimal velocities back into Eq. 2, the control matrix can also be obtained (Eq. 7).

$$\hat{\mathbf{C}} = \mathbf{Z}_{cc}^{m*} + 2\mu\mathbf{\Gamma}_c^{-2} \tag{7}$$

However, as remarked by Pizer [5], this method leaves the possibility of large motions in the uncontrolled DoFs, potentially invalidating the assumptions of linearity.

3. Formulation with extended motion constraint

Provided there exists strong enough coupling between the controlled and uncontrolled modes of motion, control forces applied through the controlled DoFs could be used to some extent to effect the motions of the uncontrolled DoFs, $\mathbf{U}_f$. This motivates an extension of the weighted global velocity constraint to include contributions from the uncontrolled DoFs (Eq. 8). Of course, $\mathbf{U}_f$ can be expressed in terms of $\mathbf{U}_c$, meaning that the additional term actually increases the restriction on $\mathbf{U}_c$, which are affected directly via the control forces, $\mathbf{F}_c$.

$$\mathbf{U}_c{}^*\mathbf{\Gamma}_c^{-2}\mathbf{U}_c + \mathbf{U}_f{}^*\mathbf{\Gamma}_f^{-2}\mathbf{U}_f \leq 1 \tag{8}$$

If the inequality given by Eq. 8 is not satisfied by the velocities demanded by unconstrained complex conjugate control, then $\mathbf{P}(\mathbf{U}_c)$ (Eq. 5) should be maximised subject to $\mathbf{U}_c{}^*\mathbf{\Gamma}_c^{-2}\mathbf{U}_c + \mathbf{U}_f{}^*\mathbf{\Gamma}_f^{-2}\mathbf{U}_f = 1$. Using the method of Lagrange multipliers (akin to Evans [3]), this is equivalent to solving Eq. 9, given the Lagrangian expression in Eq. 10. The partial derivative with respect to the complex vector, $\mathbf{U}_c$, is defined as the partial derivatives with respect to both the real and imaginary parts of $\mathbf{U}_c$ (i.e. $\frac{\partial}{\partial Re\{U_c\}} + i\frac{\partial}{\partial Im\{U_c\}}$ for each element of the velocity vector).

$$\begin{bmatrix} \frac{\partial \mathbf{Q}}{\partial \mathbf{U}_c} \\ \frac{\partial \mathbf{Q}}{\partial \mu} \end{bmatrix} = 0 \tag{9}$$

$$\mathbf{Q}(\mathbf{U}_c, \mu) = \mathbf{P}(\mathbf{U}_c) - \frac{1}{2}\mu\Big(\mathbf{U}_c{}^*\mathbf{\Gamma}_c^{-2}\mathbf{U}_c + \big[\mathbf{Z}_{ff}^{-1}(A\mathbf{X}_f - \mathbf{Z}_{fc}\mathbf{U}_c)\big]^*\mathbf{\Gamma}_f^{-2}\big[\mathbf{Z}_{ff}^{-1}(A\mathbf{X}_f - \mathbf{Z}_{fc}\mathbf{U}_c)\big] - 1\Big) \tag{10}$$

Evaluating the top row of Eq. 9 and rearranging for $\mathbf{U}_c$, yields the optimal velocities in terms of the Lagrange multiplier, μ (Eqs. 11, 12).

$$-\mathbf{B}_{cc}(\mathbf{U}_c - \frac{1}{2}\mathbf{B}_{cc}^{-1}\mathbf{X}_c^m) - \mu\big[\mathbf{\Gamma}_c^{-2}\mathbf{U}_c - (\mathbf{Z}_{ff}^{-1}\mathbf{Z}_{fc})^*\mathbf{\Gamma}_f^{-2}\mathbf{Z}_{ff}^{-1}(A\mathbf{X}_f - \mathbf{Z}_{fc}\mathbf{U}_c)\big] = 0 \tag{11}$$

$$\mathbf{U}_c^{opt} = \frac{A}{2}\Big(\mathbf{B}_{cc}+\mu\big[\mathbf{\Gamma}_c^{-2}+(\mathbf{Z}_{ff}^{-1}\mathbf{Z}_{fc})^*\mathbf{\Gamma}_f^{-2}(\mathbf{Z}_{ff}^{-1}\mathbf{Z}_{fc})\big]\Big)^{-1}\Big(\mathbf{X}_c^m+2\mu(\mathbf{Z}_{ff}^{-1}\mathbf{Z}_{fc})^*\mathbf{\Gamma}_f^{-2}\mathbf{Z}_{ff}^{-1}\mathbf{X}_f\Big) \tag{12}$$

Substituting Eq. 12 into the second row of Eq. 9, yields a scalar equation for μ (Eq. 13). The power is thus determined by Eqs. 12 and 13, along with Eq. 5, where Eqs. 14 and 15 define quantities introduced in Eq. 13.

$$\begin{aligned}&\frac{A^2}{4}\mathbf{\Omega}^*\mathbf{\Psi}(\mathbf{\Psi}\mathbf{B}_{cc}\mathbf{\Psi}+\mu\mathbf{I})^{-1}\mathbf{\Psi}\mathbf{\Gamma}_c^{-2}\mathbf{\Psi}(\mathbf{\Psi}\mathbf{B}_{cc}\mathbf{\Psi}+\mu\mathbf{I})^{-1}\mathbf{\Psi}\mathbf{\Omega}\\ &+A^2\Big(\mathbf{X}_f{}^* - \frac{1}{2}\mathbf{\Omega}^*\mathbf{\Psi}(\mathbf{\Psi}\mathbf{B}_{cc}\mathbf{\Psi}+\mu\mathbf{I})^{-1}\mathbf{\Psi}\mathbf{Z}_{fc}{}^*\Big)\mathbf{Z}_{ff}^{-1*}\mathbf{\Gamma}_f^{-2}\mathbf{Z}_{ff}^{-1}\Big(\mathbf{X}_f - \frac{1}{2}\mathbf{Z}_{fc}\mathbf{\Psi}(\mathbf{\Psi}\mathbf{B}_{cc}\mathbf{\Psi}+\mu\mathbf{I})^{-1}\mathbf{\Psi}\mathbf{\Omega}\Big)\\ &-1=0\end{aligned} \tag{13}$$

$$\mathbf{\Psi}^{-2} = \mathbf{\Gamma}_c^{-2} + (\mathbf{Z}_{ff}^{-1}\mathbf{Z}_{fc})^*\mathbf{\Gamma}_f^{-2}\mathbf{Z}_{ff}^{-1}\mathbf{Z}_{fc} \tag{14}$$

$$\mathbf{\Omega} = \mathbf{X}_c^m + 2\mu(\mathbf{Z}_{ff}^{-1}\mathbf{Z}_{fc})^*\mathbf{\Gamma}_f^{-2}\mathbf{Z}_{ff}^{-1}\mathbf{X}_f \tag{15}$$

It is interesting to note that, in contrast with the foundational theory presented in Section 2, the control matrix is not so easily obtained, due to the presence of the extra term in the second bracket of Eq. 12. However, since the control forces and the optimal velocities are known, numerical methods could be used to obtain at least an approximation to this matrix, if necessary.

4. Numerical solution

Whereas the constrained systems considered in [4] depend only on the radiation damping coefficients, $\mathbf{B}$, and the excitation forces, $\mathbf{X}$, the systems under consideration in this paper are additionally dependent on the hydrostatic and inertial properties, due to the interaction of the controlled motions with the uncontrolled motions (Eqs. 1 - 4). Whilst the inertial properties derive from the mass distribution of the body (or collection of bodies) under consideration, the hydrodynamic and hydrostatic properties may be obtained from physical experiments, or as is now increasingly common, numerically by use of a radiation/diffraction code, such as WAMIT [10], which has been used in this study. Generalised modes [11] allow this technique to be applied to an arbitrary set of degrees of freedom, an example of which could be a collection of mechanically interlinked bodies, as well as to more standard applications, such as a wave energy converter array.

As with the analysis given in [4], it is useful to diagonalise the symmetric matrix $\mathbf{\Psi B}_{cc}\mathbf{\Psi}$, using its matrix of eigenvectors, $\mathbf{Q}$ (Eq. 16), which results in Eq. 17. Since $\mathbf{B}_{cc}$ and $\mathbf{\Psi}$ are symmetric, positive definite matrices, the elements of $\mathbf{\Lambda}$, $\lambda_i > 0$ for all i. Therefore, the poles of Eq. 17 all occur at negative μ values, which means there exist at most $2N$ real roots, of which one at most is real and positive.

$$\mathbf{\Lambda} = \mathbf{Q}^* \mathbf{\Psi B}_{cc} \mathbf{\Psi Q} \tag{16}$$

$$\begin{aligned} g(\mu) \equiv \frac{1}{4}\mathbf{\Omega}^* \mathbf{\Psi Q}(\mathbf{\Lambda} + \mu\mathbf{I})^{-1}\mathbf{Q}^* \mathbf{\Psi \Gamma}_c^{-2} \mathbf{\Psi Q}(\mathbf{\Lambda} + \mu\mathbf{I})^{-1}\mathbf{Q}^* \mathbf{\Psi \Omega} \\ + \Big(\mathbf{X}_f{}^* - \frac{1}{2}\mathbf{\Omega}^* \mathbf{\Psi Q}(\mathbf{\Lambda} + \mu\mathbf{I})^{-1}\mathbf{Q}^* \mathbf{\Psi Z}_{fc}{}^*\Big)\mathbf{Z}_{ff}^{-1*}\mathbf{\Gamma}_f^{-2}\mathbf{Z}_{ff}^{-1}\Big(\mathbf{X}_f - \frac{1}{2}\mathbf{Z}_{fc}\mathbf{\Psi Q}(\mathbf{\Lambda} + \mu\mathbf{I})^{-1}\mathbf{Q}^* \mathbf{\Psi \Omega}\Big) \\ = \frac{1}{A^2} \end{aligned} \tag{17}$$

When $\mu = 0$, Eq. 12 reverts to the optimal velocities for the unconstrained case. As defined in Eq. 10, $\mu > 0$, which can only be the case when $A > A_c = \sqrt{\frac{1}{g(0)}}$; the constraint only becomes active when $A > A_c$. In this case, of the $2N$ complex roots of Eq. 17, still one at most can be real and positive, corresponding to a valid solution. As $\mu \to \infty$, $g(\mu) \to A^2 \mathbf{X}_f^* (\mathbf{Z}_{ff}^{-1})^* \mathbf{\Gamma}_f^{-2} \mathbf{Z}_{ff}^{-1} \mathbf{X}_f \equiv C$, and if $C > 1$, $\mathbf{U}_c{}^* \mathbf{\Gamma}_c^{-2} \mathbf{U}_c + \mathbf{U}_f{}^* \mathbf{\Gamma}_f^{-2} \mathbf{U}_f > 1$ for all $\mu > 0$, signifying that the constraint (8) cannot be satisfied. In physical terms, this corresponds to an insufficient strength of coupling between the controlled and uncontrolled modes of motion; the motions of the uncontrolled modes will always lead to violation of the constraint, regardless of the forces applied through the controlled modes of motion. Therefore, it is imperative that the nature of the application is considered in choosing the weightings, $\mathbf{\Gamma}_f$, before applying constraint (8). It is interesting to note that the presence of a solution is directly dependent only on properties of the uncontrolled modes, and the wave amplitude. However, the equations of motion (Eq. 1) link these properties of the free modes to the coupling between the controlled and free modes. Whilst Eq. 17 is a scalar equation, for systems with large N it is most practical to solve for μ numerically.

5. Applications to a solo duck

The solo duck is a single body wave energy device, derived from the originally proposed spine-based system [12]. Though initially designed to extract power through its pitch rotations, allowing power extraction via multiple degrees of freedom can benefit the total absorbed power, whilst reducing the cost of rigidly fixing degrees of freedom in a harsh sea environment. Furthermore, it may reduce costs further to concede control of certain degrees of freedom, especially if there were no significant negative impact on the power extraction. In this section, the methods described in this paper are applied to a solo duck whose

shape is adapted from that of the D0018 Medium Beak Duck in [13]. Figure 1 shows a side view of the duck used in this study, with the axes defining the body motions overlaid. Seven cylindrical ballast tubes of 1.27m diameter, each of constant density, permit the desired mass distribution, and are defined in Table 1. The radial positions are defined from the centre of rotation, and angular positions defined clockwise from the part of the centreline joining the centre of rotation and the beak tip (the pointed edge of the duck). The centreline is orientated at 36° to the horizontal, the distance from the centre of rotation to the beak tip along the centreline is 11.8m, and a duck width of 29.5m is presented to the incoming waves. The portion of the duck surrounding the ballasts has a mass of $1.226\text{x}10^6$kg, giving an average density of 337kgm^{-3}. This results in a mean waterline 4.12m above the centre of rotation, and gives a duck that is statically stable in roll and pitch. Given the similarity in size of the duck employed in this study to the duck used in [4], the same constraint weightings are used - β_i of 2.5m for the translational motions, 0.5rad for pitch, and 0.2rad for roll and yaw, where the velocity constraint weightings, $\gamma_i = \omega\beta_i$ are the diagonal elements of $\mathbf{\Gamma}$.

Except for a single case, in which the wave amplitude is clearly stated, the incident waves used in this section are of unit amplitude.

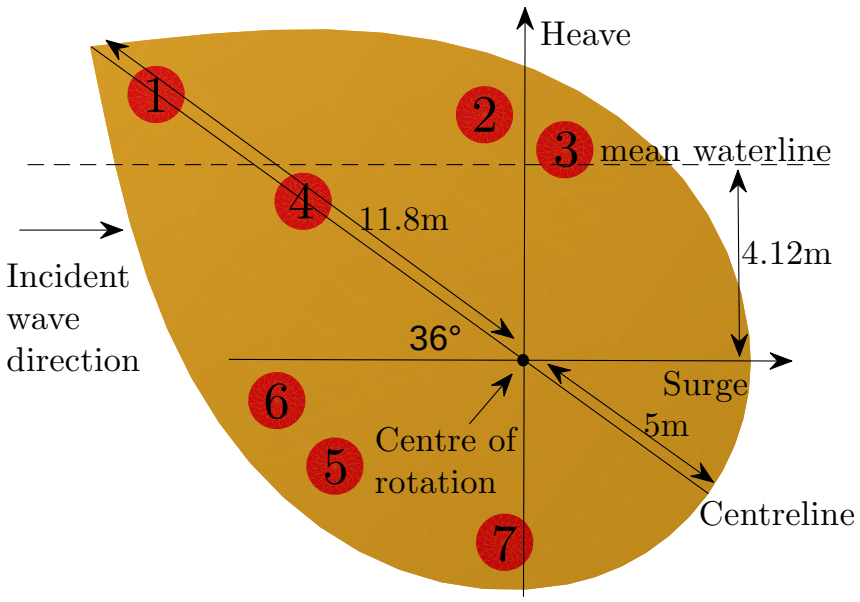

Figure 1: Side view of the solo duck in its equilibrium configuration, with the seven ballast tube locations. Sway is defined into the page, with the axes centred halfway along the duck's width.

Ballast index	Mass / kg	Radial position / m	Angular position / °
1	0	10	0
2	456000	5.5	45
3	312000	4.75	65
4	134000	6	0
5	0	4.75	-65
6	56000	5.5	-45
7	752500	4	-120

Table 1: Definitions of the masses and positions of the seven ballast tubes.

Under head-on waves, the symmetry of the device reduces the solo duck to a three degree of freedom system. Studying a similar solo duck system, Pizer [5] noted that releasing control of the surge degree of freedom resulted in a larger reduction in power than by releasing heave or pitch, for whom the reduction was small. Consequently, a solo duck with control over just surge and heave motions may provide comparable performance to a system with pitch also controlled. We adopt this example to highlight the potential importance of using the extended constraint introduced in Section 3. Surge and heave are controlled, whilst the pitch degree of freedom is uncontrolled. Wavefronts are parallel to the axis of pitch rotation, and 1m and 2m wave amplitudes are considered. (Given the periods that are likely to accompany them in a real sea climate, these wave amplitudes are not thought to be large enough to hinder the use of a linear model.)

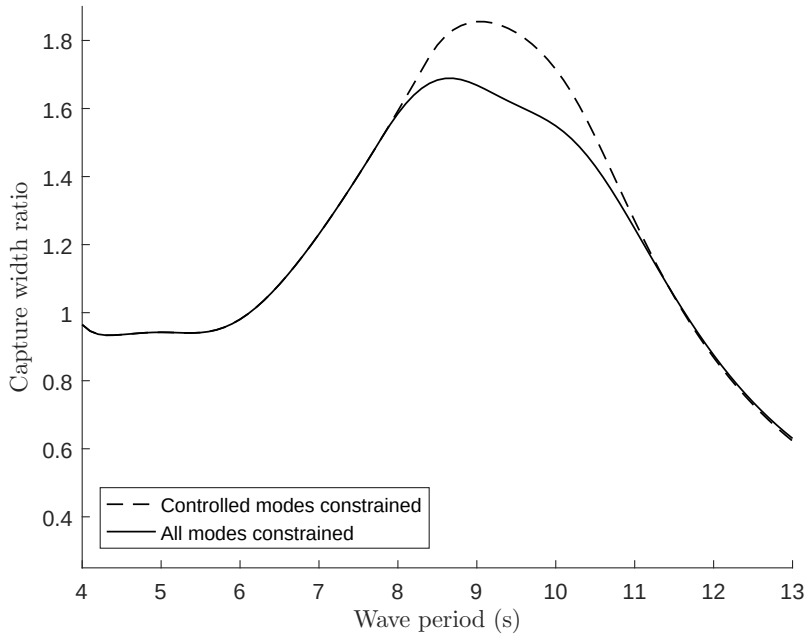

Figure 2: The impact of extending the motion constraint to uncontrolled degrees of freedom on the capture width ratio for a solo duck. Surge and heave motions controlled, 1m wave amplitude.

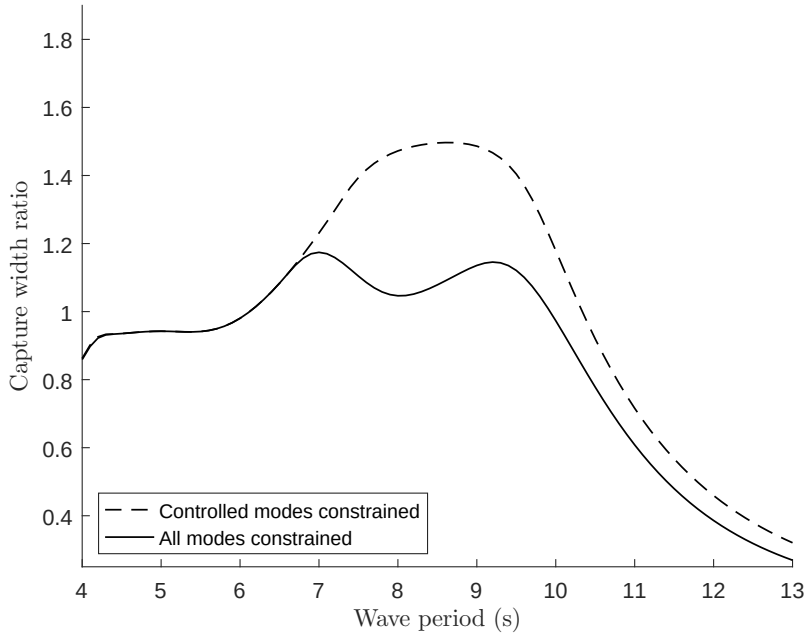

Figure 3: The impact of extending the motion constraint to uncontrolled degrees of freedom on the capture width ratio for a solo duck. Surge and heave motions controlled, 2m wave amplitude.

Especially around the peak in capture width ratio, whether or not the motion constraint is enforced on all degrees of freedom, or just those of surge and heave, makes a significant difference. Under 1m incident waves, a small difference in capture width ratio is present between 8 and 11s wave periods (Fig. 2). For 2m wave amplitudes, which are not unlikely to be encountered in a real wave climate, the difference extends to a much wider range of wave periods, and is more significant (Fig. 3). Capture width ratio is reduced from a peak value of around 1.5 to a peak value around 1.2. Note also that the peak in capture width ratio with both versions of the constraint is lower in the 2m waves (than in the 1m waves) because a greater departure from the unconstrained control case is required in order to satisfy the motion constraints. (In the unconstrained case, one would expect equivalent capture width ratio plots, since both the extracted power and the power in the waves scale with the square of the wave amplitude, under linear theory.) In other words, the constraint more severely curtails the motions in waves of larger amplitude. It is for this reason, along with the fact that the motions demanded by complex conjugate control strategies tend to increase for longer waves, that the power in the 2m wave case is also reduced

over a wider range of wave periods when the constraint is extended, than with the 1m waves.

In the case with 2m waves shown here, that follows the method from Section 2, the unconstrained pitch motions reach unrealistically high values (around 2rad for a wave period of 9.6s), which violates the assumption of linearity (Fig. 4). Extending the constraint to also restrict the pitch motions unsurprisingly results in reduced pitch motions for wave periods above 7s, with surge excursions reduced similarly. Interestingly, heave motions actually increase slightly for wave periods above 8.5s.

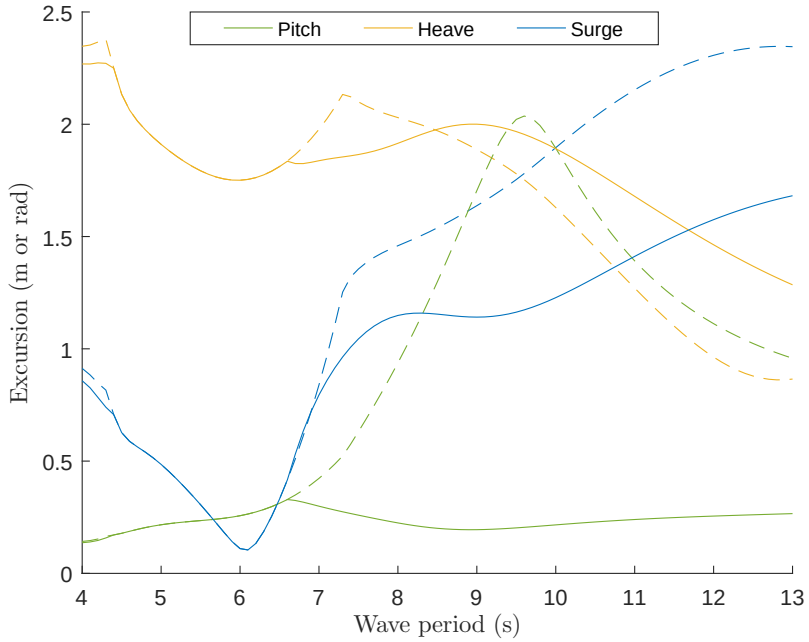

Figure 4: The impact of extending the motion constraint to uncontrolled degrees of freedom on motions on the surge, heave and pitch body motions. Surge and heave motions controlled, 2m wave amplitude. Dotted lines: Constraint applied only to controlled modes. Solid lines: Constraint applied to all modes.

In general, the extended constraint (Eq. 8) can only be satisfied if the controlled modes have enough influence on the uncontrolled modes via the hydrodynamic, hydrostatic and inertial coupling, to restrict the motions sufficiently. In the case of the solo duck under head-on waves considered above, the constraints on the out-of-plane motions (in sway, roll and yaw) are trivially satisfied since they are not excited by the waves. The constraints on the in-plane motions can be satisfied because coupling between the pitch degree of freedom and the surge and heave degrees of freedom is sufficiently strong. However, oblique waves excite the out-of-plane motions, sometimes to the extent that no amount of force imparted through the surge and heave motions is sufficient to restrict the

out-of-plane motions in accordance with the weighted constraint. Fig. 5 shows that between 7 and 8s wave periods, and for wave angles greater than 10°, a solution that satisfies the extended constraint does not exist when only surge, heave and pitch are controlled. In this case, the constraint violation is due to resonant response in sway and roll, which are not coupled strongly enough to surge, heave and pitch.

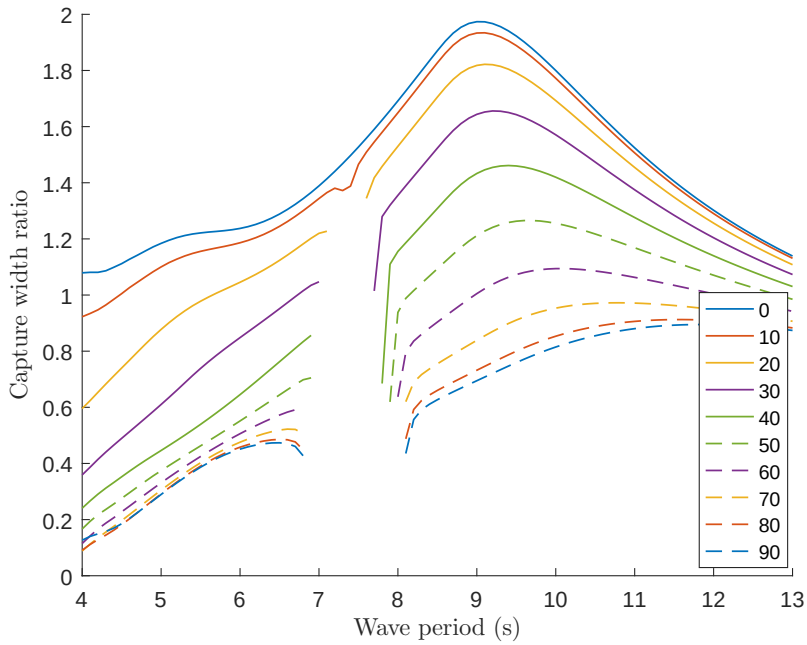

Figure 5: Capture width ratio of a solo duck with uncontrolled sway, roll and yaw modes. Motion constraint applied to all modes, 1m wave amplitude. Legend defines the data lines for each wave heading, in degrees.

Bolstering this strategy with (direct) control over the sway motions also increases the degree of indirect control over the roll motions via coupling. Solutions are now found for all wave periods, with heading angles up to and including 60°, but there still remain regions in which no solution exists for greater wave angles (Fig. 6).

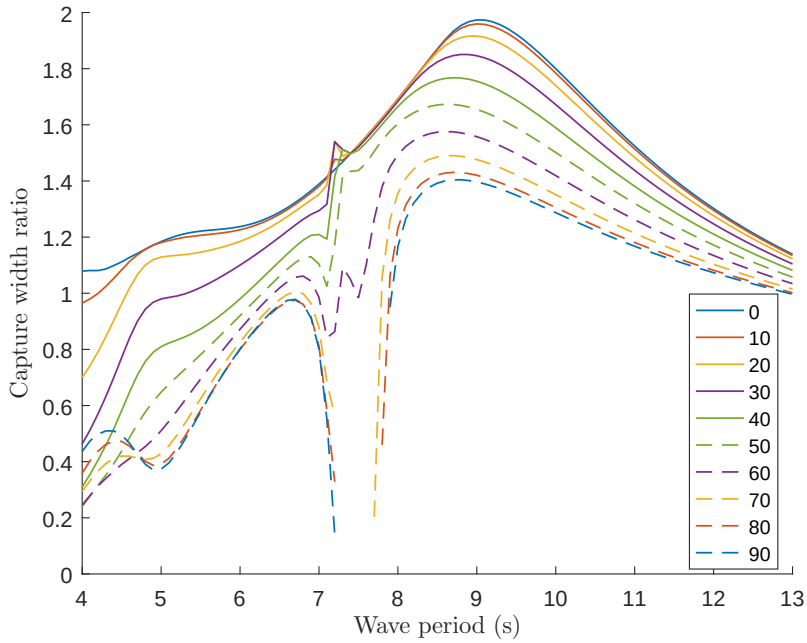

Figure 6: Capture width ratio of a solo duck with uncontrolled roll and yaw modes. Motion constraint applied to all modes, 1m wave amplitude. Legend defines the data lines for each wave heading, in degrees.

The greater range of solutions is largely due to the hydrodynamic coupling between the sway and roll modes, enabling control forces applied through sway to restrict the motion in roll. However, this strategy results in larger sway excursions, increasingly so for more oblique wave headings, which ultimately causes constraint violation for wave angles above 60°. Fig. 7 shows the limiting case with 60° waves, in which control forces are just about able to sufficiently restrict the roll motions at the expense of increased sway excursions, without violating the motion constraint (Eq. 8). Fig. 8 shows the motion amplitudes of the undamped and unstiffened system (i.e. all modes uncontrolled) with a 60° wave heading; the sway and roll motions are resonant together around 7.5s. In particular, the roll amplitude exceeds its individual weighting (β) between 7 and 8s wave periods, indicating constraint violation, whilst the sway excursion is considerably below its corresponding weighting, giving the necessary buffer for some of the excess motion in roll to be converted to sway motion. Fig. 6 also highlights that the power tends towards a large negative value either side of the region containing no solutions to the Lagrange problem. As this region is neared from lower or higher wave periods, the approaching resonance of the roll motions increasingly necessitates counteractive force provision in order to satisfy the weighted global constraint. This comes at the expense of power generation, but prevents the constraint being violated. In turn, this causes increased sway

excursions, and further reduces power generation until eventually, there are no solutions to the constraint, regardless of the decrease in power.

Of the 62 (6 + 15 + 20 + 15 + 6) combinations of controlled modes of the solo duck (excluding the cases where all are controlled or all are uncontrolled), the non-existence of solutions has been found at most to involve a narrow range of wave periods and less than the full range of wave angles. In those cases, the peaks in capture width ratio generally lie outside the period-angle combinations of the non-existence regions.

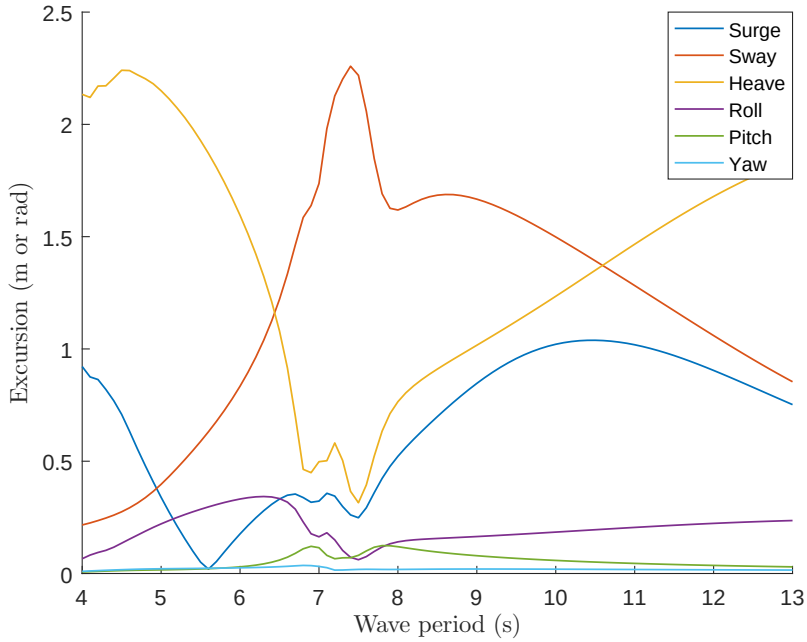

Figure 7: Motions of the solo duck in 60° oblique waves, optimised for power under the extended global motion constraint. Controlled modes: surge, sway, heave, pitch.

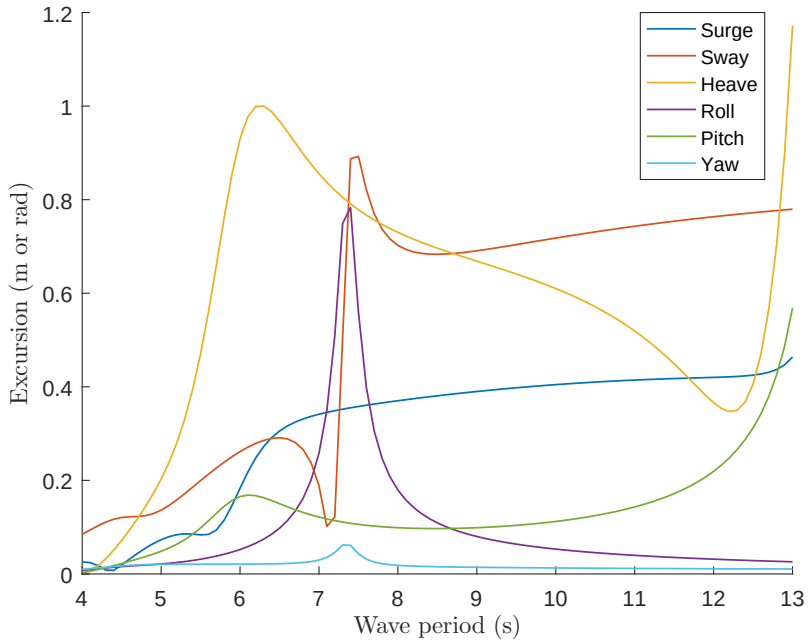

Figure 8: Motions of the undamped and unstiffened solo duck in 60° oblique waves. Controlled modes: surge, sway, heave, pitch.

Under head-on waves, where the simplified system has three degrees of freedom, locking a degree of freedom does not necessarily cause a significant reduction in performance [4]. From a two degree of freedom system, releasing (i.e. changing it from fixed, to free but uncontrolled) the third degree of freedom results in a loss in power, which is much greater when surge is released rather than heave or pitch [5]. Of course, that study [5] left open the possibility of large motions in the uncontrolled degree of freedom. However, a similar trend is found in the duck system studied here under the impact of the extended motion constraint. Under head-on waves (a wave heading of 0°), conceding control of surge results in a greater loss of power than conceding control of heave or pitch (Fig. 9). The peak capture width ratio value of 1.97 reduces only to 1.79 in conceding control of heave. Despite some additional loss of bandwidth, this may still provide an advantage if the systems required to control the heave (or pitch) degree of freedom are costly.

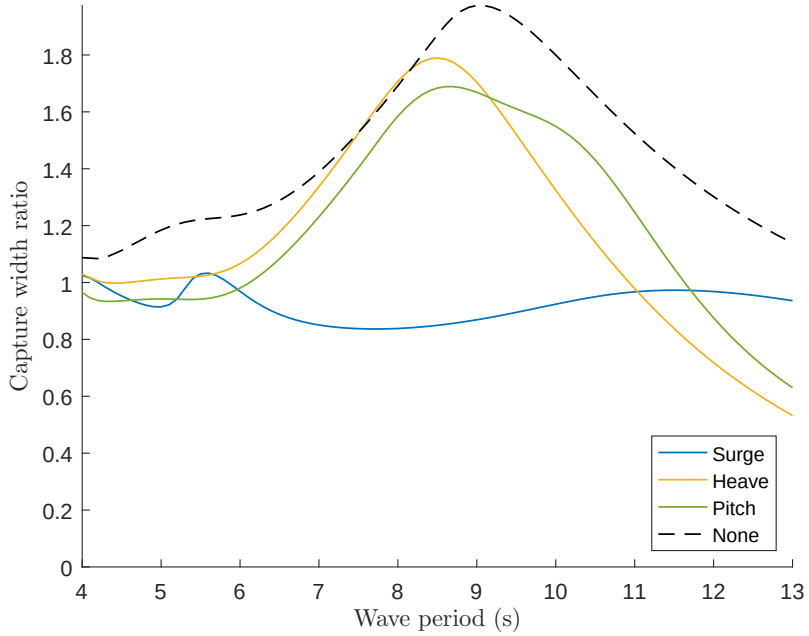

Figure 9: Capture width ratio of the solo duck in head-on waves, with control of each in-plane degree of freedom conceded in turn. Wave angle: 0°; wave amplitude: 1m. Legend indicates in which degree of freedom control has been conceded, if any. (Note that the three out-of-plane degrees of freedom do not affect this system because of the symmetry of the device, and so have not been plotted.)

Whilst out-of-plane degrees of freedom (sway, roll and yaw) do not affect the power capture with a 0° wave heading due to the plane of symmetry of the duck, it is not the case that the in-plane degrees of freedom do not affect the power capture with a 90° wave heading. In transitioning between 0° and 90° wave headings, the roles of surge and sway broadly interchange. In head-on waves, conceding control of surge results in a significant power reduction across a wide range of wave periods, whilst conceding control of sway has no effect. Conversely, in 90° waves, conceding control of sway reduces power significantly, whereas little effect is had by conceding control of surge (Fig. 10). Conceding control of heave or pitch tends to diminish the power across the full range of wave angles, especially in longer wave periods, but the power reduction is relatively insignificant (Fig. 9). Conceding control of yaw or roll does not have any significant impact on power in wave angles close to either end of the range (Figs. 9, 10), and causes only modest reductions in power for intermediate wave angles (e.g. at 30°, see Fig. 11), the majority of which occurs at lower wave periods. In fact, conceding control of roll actually increases power for wave periods between 7.3 and 8.5s, and for intermediate angles, compared to the case in which all degrees of freedom are controlled. This may seem counter-

intuitive, but the situation (greater power with control over fewer degrees of freedom) is possible if a greater shift away from true optimality (by providing extra damping) is required, in order to satisfy the constraint in the case where all six degrees of freedom are controlled.

Considering that a real deployment location may only experience a small range of incident wave angles, the device is likely to be set at an angle of around 30° since this enables a very wide bandwidth, without sacrificing much in peak power (Figs. 9, 11, see also [4]). In this light, conceding control of heave, pitch or roll seem to be least detrimental to performance, though conceding control of yaw may be a better option towards higher wave periods.

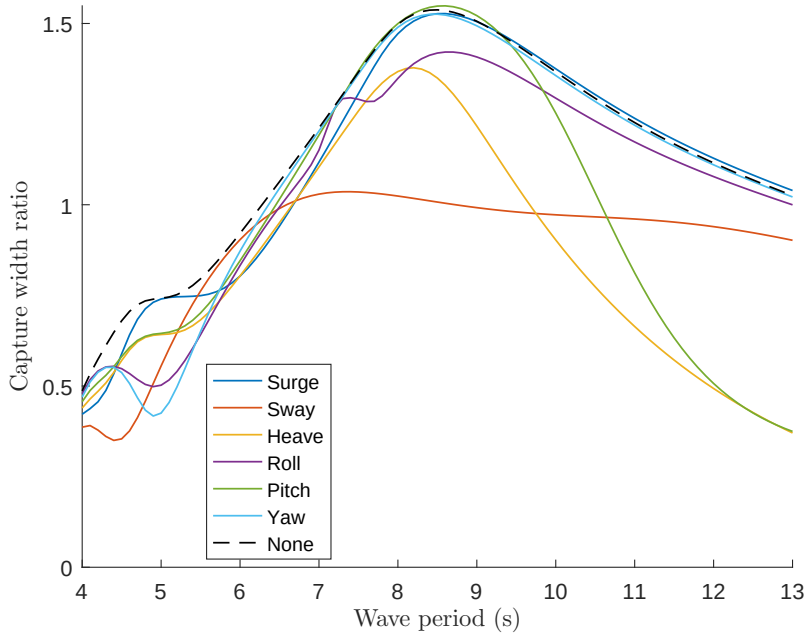

Figure 10: Capture width ratio of the solo duck in 90° incident waves, with control of each degree of freedom conceded in turn. Legend indicates in which degree of freedom control has been conceded, if any.

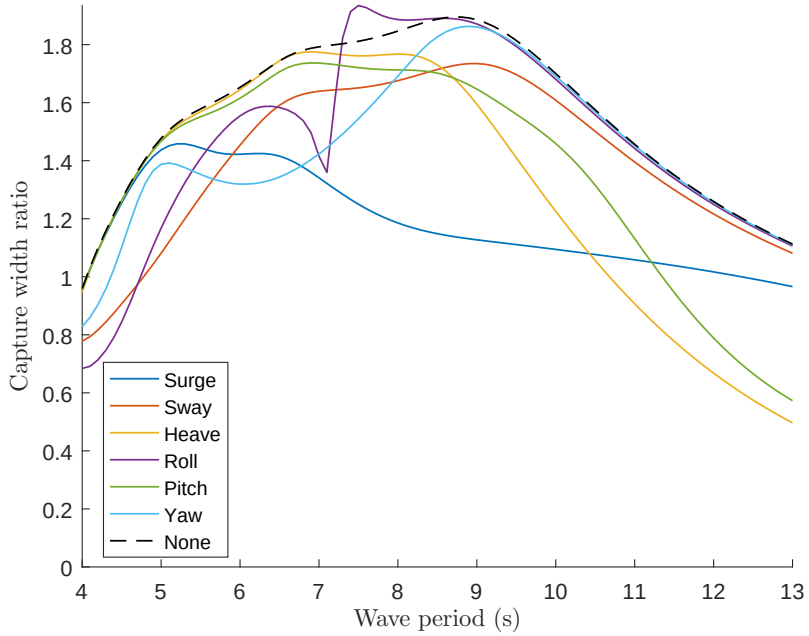

Figure 11: Capture width ratio of the solo duck in 30° incident waves, with control of each degree of freedom conceded in turn. Legend indicates in which degree of freedom control has been conceded, if any.

Furthermore, conceding control of two degrees of freedom can even retain the majority of the power capture across a slightly narrowed band of wave periods (see the red and green lines in Fig. 12). However, sacrificing control of both heave and pitch results in a much reduced capture width ratio (see the blue line in Fig. 12), inferring that when just heave or pitch is uncontrolled, control of the other is necessary to compensate. Should it be desired that three degrees of freedom are uncontrolled, it is best to retain control over the translational degrees of freedom. This case compares favourably to the one in which all degrees of freedom are controlled (see the purple line in Fig. 12). Conversely, conceding control of the translational degrees of freedom, but retaining control of the rotational degrees of freedom, results in a large loss of power across a wide range of wave periods (see the light blue line in Fig. 12).

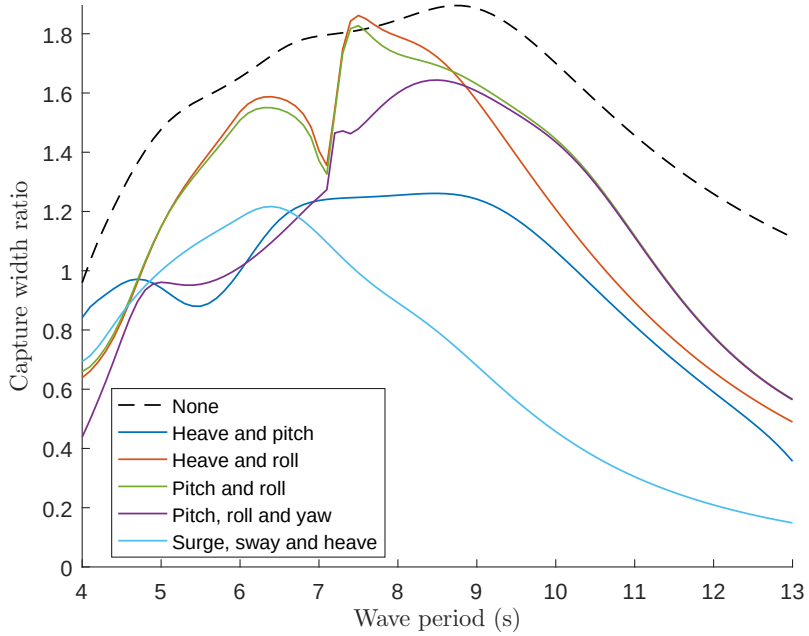

Figure 12: Capture width ratio of the solo duck in 30° incident waves, with a selection of better performing combinations of uncontrolled modes. Legend indicates in which degrees of freedom control has been conceded, if any.

6. Conclusions

In reference [4], a method was derived to apply complex conjugate control with a global motion constraint. That constraint consisted of a set of weightings associated with only controlled modes of motion. The present study has extended that constraint to also include weightings associated with uncontrolled modes of motion.

The new method was then applied to a six degree-of-freedom solo duck, initially focussing on an in-plane case where there was no direct control over pitching. That case demonstrated that the use of the extended constraint can often be essential, in order to avoid unrealistic motions and significant overestimation of the power.

However, more generally, care should be taken when applying the extended constraint, since its satisfaction relies upon sufficient levels of hydrodynamic, hydrostatic and inertial coupling between the controlled and uncontrolled degrees of freedom. The presence of a solution is dictated by the wave amplitude, and properties of only the uncontrolled modes, although a subset of those properties can be related to the coupling between the controlled and uncontrolled modes via the equations of motion. With the constraint weightings, wave amplitude and duck geometry considered in this paper, regions of solution non-existence

were confined to only a narrow range of wave periods, and importantly were situated away from the peaks in capture width ratio.

With regards to the cost savings (particularly of the power take-off system) that may accompany a relinquishment of control of certain degrees of freedom, a number of conclusions can be made for the solo duck.

- In head-on waves, control can be conceded in either heave or pitch (but not both) without significant reductions in power. Surge control should be retained.
- In oblique waves, conceding control of roll can actually result in increases in capture width ratio for certain wave period ranges.
- In 30° oblique waves, there are several key permutations of control concessions, which result in only small performance reductions:
  - Conceding control of heave, roll or pitch (leaving 5 controlled modes),
  - Conceding control of heave and roll or pitch and roll (leaving 4 controlled modes),
  - Conceding control of roll, pitch and yaw (leaving 3 controlled modes).
- In general, control of only one of the heave and pitch modes at most should be sacrificed; conceding control of both results in significantly lowered capture width ratio.

Acknowledgement

This work was supported by a studentship provided by the EPSRC through the Wind and Marine Energy Systems Centre for Doctoral Training [award reference 1809924].

References

[1] J. Falnes, Radiation impedance matrix and optimum power absorption for interacting oscillators in surface waves, Applied Ocean Research 2 (1980) 75–80. doi:10.1016/0141-1187(80)90032-2.

[2] P. Nebel, Maximizing the efficiency of wave-energy plant using complex-conjugate control, Proceedings of the Institution of Mechanical Engineers, Part I: Journal of Systems and Control Engineering 206 (1992) 225–236. doi:10.1243/PIME_PROC_1992_206_338_02.

[3] D. V. Evans, Maximum wave-power absorption under motion constraints, Applied Ocean Research 3 (1981) 200–203. doi:10.1016/0141-1187(81)90063-8.

[4] D. J. Pizer, Maximum wave-power absorption of point absorbers under motion constraints, Applied Ocean Research 15 (1993) 227–234. doi:10.1016/0141-1187(93)90011-L.

[5] D. J. Pizer, Numerical modelling of wave energy absorbers, Edinburgh Research Archive (1994, accessed on 28/03/2020).
URL http://hdl.handle.net/1842/23532

[6] U. A. Korde, Wave energy conversion under constrained wave-by-wave impedance matching with amplitude and phase-match limits, Applied Ocean Research 90 (2019) . doi:10.1016/j.apor.2019.101858.

[7] J. Falnes, Maxiumum wave-energy absorption by oscillating systems consisting of bodies and water columns with restricted or unrestricted amplitudes, Proceedings of The Tenth International Offshore and Polar Engineering Conference (2000) 420–426.
URL https://www.onepetro.org/conference-paper/ISOPE-I-00-061

[8] D. Richardson, Multi-axis point absorber wave energy converters, Ph.D. thesis, Lancaster University (2019). doi:10.17635/lancaster/thesis/616.

[9] J. Wu, Y. Yao, N. Chen, H. Yu, W. Li, M. Goeteman, Performance analysis of solo duck wave energy converter arrays under motion constraints, Energy 139 (2017) 155–169. doi:10.1016/j.energy.2017.07.152.

[10] WAMIT User Manual (v7.2), WAMIT Inc., http://www.wamit.com/manual.htm, Accessed: 28/03/2020.

[11] J. N. Newman, Wave effects on deformable bodies, Applied Ocean Research 16 (1994) 47–59. doi:10.1016/0141-1187(94)90013-2.

[12] S. H. Salter, Wave power, Nature 249 (1974) 720–724. doi:10.1038/249720a0.

[13] D. C. Jeffrey, D. J. E. Richmond, S. H. Salter, J. R. M. Taylor, Second year interim report on Edinburgh wave power project: "Study of Mechanisms for Extracting Power from Sea Waves", Edinburgh Research Archive (1978, accessed on 28/03/2020).
URL http://hdl.handle.net/1842/23410